RESEARCH ARTICLE

Brain Pathology

Expression pattern of mitochondrial respiratory chain enzymes in skeletal muscle of patients with mitochondrial myopathy associated with the homoplasmic m.14674T>C variant

Sara Roos[1] | **Carola Hedberg-Oldfors[1]** | **Kittichate Visuttijai[1]** | **My Stein[2]** | **Gittan Kollberg[1]** | **Ólöf Elíasdóttir[3]** | **Christopher Lindberg[3]** | **Niklas Darin[4]** | **Anders Oldfors[1]**

[1]Department of Laboratory Medicine, Institute of Biomedicine, University of Gothenburg, Gothenburg, Sweden

[2]Department of Pediatrics, Helsingborg Hospital, Helsingborg, Sweden

[3]Department of Neurology, Neuromuscular Center, Sahlgrenska University Hospital, Gothenburg, Sweden

[4]Department of Pediatrics, Institute of Clinical Sciences, University of Gothenburg, Gothenburg, Sweden

Correspondence
Sara Roos, Department of Laboratory Medicine, Institute of Biomedicine, University of Gothenburg, Gothenburg, Sweden.
Email: sara.m.roos@vgregion.se

Abstract

Two homoplasmic variants in tRNA^{Glu} (m.14674T>C/G) are associated with reversible infantile respiratory chain deficiency. This study sought to further characterize the expression of the individual mitochondrial respiratory chain complexes and to describe the natural history of the disease. Seven patients from four families with mitochondrial myopathy associated with the homoplasmic m.14674T>C variant were investigated. All patients underwent skeletal muscle biopsy and mtDNA sequencing. Whole-genome sequencing was performed in one family. Western blot and immunohistochemical analyses were used to characterize the expression of the individual respiratory chain complexes. Patients presented with hypotonia and feeding difficulties within the first weeks or months of life, except for one patient who first showed symptoms at 4 years of age. Histopathological findings in muscle included lipid accumulation, numerous COX-deficient fibers, and mitochondrial proliferation. Ultrastructural abnormalities included enlarged mitochondria with concentric cristae and dense mitochondrial matrix. The m.14674T>C variant in *MT-TE* was identified in all patients. Immunohistochemistry and immunoblotting demonstrated pronounced deficiency of the complex I subunit NDUFB8. The expression of MTCO1, a complex IV subunit, was also decreased, but not to the same extent as NDUFB8. Longitudinal follow-up data demonstrated that not all features of the disorder are entirely transient, that the disease may be progressive, and that signs and symptoms of myopathy may develop during childhood. This study sheds new light on the involvement of complex I in reversible infantile respiratory chain deficiency, it shows that the disorder may be progressive, and that myopathy can develop without an infantile episode.

KEYWORDS
homoplasmic mt-tRNA^{Glu} variant, mitochondrial myopathy, mtDNA, reversible infantile respiratory chain deficiency, whole genome sequencing

1 | INTRODUCTION

Mitochondrial disorders are a heterogeneous group of disorders associated with a wide range of clinical phenotypes, which arise due to dysfunction of the mitochondrial respiratory chain. Mitochondrial diseases with childhood-onset are often severe and progressive, with substantial morbidity and mortality. However, there are rare forms that show remarkable spontaneous recovery. Two homoplasmic variants in tRNA^{Glu} (m.14674T>C/G) have been shown to be associated with reversible infantile respiratory chain deficiency [1–3]. These children present with hypotonia, hyporeflexia, lactic acidosis, and severe muscle weakness from early infancy and often require assisted ventilation, features similar to those seen in the fatal infantile forms [4], but they recover spontaneously, usually within a few months. Muscle biopsy demonstrates complex IV (cytochrome *c* oxidase, COX)-deficient fibers and mitochondrial proliferation, and biochemically a combined complex I/IV deficiency is usually seen [1–6]. Electron microscopy findings include abnormal mitochondria, but a more detailed description of ultrastructural abnormalities is sparse. This entity has been given the name reversible infantile respiratory chain deficiency. The mechanism of the sudden onset and spontaneous recovery has not yet been determined, but the m.14674T>C/G is thought to impair mitochondrial translation. As most individuals who are homoplasmic for m.14674T>C/G do not show signs or symptoms of muscle disease at any stage, it has been suggested that additional heterozygous variants in nuclear genes interacting with mt-tRNA^{Glu} may be a prerequisite for disease manifestation [7].

In this study, we present clinical and laboratory findings in seven individuals from four families with mitochondrial myopathy associated with the homoplasmic m.14674T>C variant. Longitudinal follow-up data indicate that myopathic features may persist into adolescence/adulthood and may even deteriorate in some cases, and that signs and symptoms of myopathy may develop insidiously during childhood. Furthermore, this study sought to further characterize the expression of the individual mitochondrial respiratory chain complexes at different stages of this disease, to widen the understanding of underlying pathological mechanisms.

2 | MATERIALS AND METHODS

2.1 | Patients

This study included seven patients (P1–P7) from four families with mitochondrial myopathy associated with the homoplasmic m.14674T>C variant (Figure 1 and Table 1). Detailed clinical information for each patient is provided in the supplement file. All patients were Caucasians, but from different ethnic groups (Swedish and Iraqi). Four of the patients (P1-P3, P5) have been partly reported previously [1, 6–8,].

All protocols were approved by the Regional Ethical Review Board in Gothenburg.

2.2 | Laboratory analyses

Morphological and enzyme histochemical analyses of fresh frozen skeletal muscle biopsy specimens were performed according to established protocols [9]. For estimation of the proportion of COX-deficient fibers, double staining of COX and succinate dehydrogenase (SDH)

FIGURE 1 Pedigrees of the four investigated families. Filled symbol represents individuals with mitochondrial myopathy associated with the homoplasmic m.14674T>C variant, dot represents carrier, # represents clinically examined individual. In Family 4, two disease-causing genetic variants (*SYNE1*, c.25448G>A and m.14674T>C) are present. %, amount of m.14674T>C; M, mutated *SYNE1* sequence; P, patient; R, relative; WT, normal *SYNE1* sequence

TABLE 1 Clinical findings

Family	Patient age at onset	Infantile clinical presentation	Longitudinal follow-up	Family history
1	P1/M 1 mo	1 mo: Vomiting, feeding difficulties, and failure to thrive 2 mo: Pneumonia and sepsis, muscle weakness and generalized hypotonia Tube feeding because of swallowing difficulties. No ventilatory support Increased urinary excretion of lactate, Blood lactate 4X unl Serum CK increased	Exercise intolerance throughout childhood and adolescence 1.5 yr: Slightly delayed gross motor development, walked unsupported 2.5 yr : Motor function, muscle strength and cognitive development were normal 18 yr: Reduced exercise capacity (40% of normal). Exercise-induced hyperlactatemia. Motor function, muscle strength at rest and deep tendon reflexes normal. Ophthalmological and cardiological investigations normal. Serum CK slightly elevated	Sister with high-functioning autism Mother (I:2, Figure 1) healthy, without signs or symptoms of myopathy or exercise intolerance
2	P2/M 1 mo	1 mo: Increasing irritability and lethargy 2 mo: Generalized muscular hypotonia, feeding difficulties, and failure to thrive Blood lactate 12X unl Serum CK mildly increased Mild liver involvement. A liver biopsy at 4 mo with mild steatosis but normal enzyme histochemical COX	Blood lactate has been normal after rise in neonatal period 2 yr : Normal mental and fine motor development. Delayed gross motor development 3 yr: Walked unsupported 5 yr: Improved with slight muscle weakness 14 yr: Decreased muscle strength with walking difficulties, unable to run. Serum CK 16X–25X unl 32 yr: Decline in ambulation. 6-min walk test with reduced capacity (65% of expected). Exercise intolerance with myalgia and muscle cramps. Serum CK 6X unl	Mother (I:2, Figure 1) without any symptoms of myopathy
	P3/M 1 mo	1 mo: Respiratory syncytical virus infection with feeding difficulties Muscular hypotonia, swallowing difficulties, and respiratory failure. Transient CPAP treatment Massive urine excretion of lactate (110X unl). Blood lactate 4X unl Serum CK normal Gastrostomy feeding until 2 yr	1.5 yr: Slightly delayed gross motor development, walked unsupported. Delayed speech development because of dysarthria 12 yr: Residual muscle weakness with a positive Gower's sign, exercise intolerance, decline in ambulation. Mild ptosis, increased lumbar lordosis, weak tendon reflexes. Serum CK normal Cardiological and ophthalmological investigations normal	Maternal nephew of P2 Mother (II:2, Figure 1) without any symptoms of myopathy
	P4/F 2 mo	2 mo: Feeding difficulties, dysphagia, and failure to thrive. Tube feeding was required for nutrition. Muscular hypotonia Blood lactate 2X unl Serum CK normal	Slightly delayed gross motor and speech development 3.5 yr: Exercise intolerance, dysarthria, difficulties swallowing solid food. Motor function, muscle strength at rest and deep tendon reflexes were normal Normal blood lactate, serum CK 1.2X unl	Maternal half-sister of P3 Mother (II:2, Figure 1) without any symptoms of myopathy
3	P5/F 3 wk	3 wk: Failure to thrive with poor feeding, vomiting and lactic acidosis 3 mo: Profound muscular hypotonia and swallowing difficulties which required gastrostomy	19 mo: Slightly delayed early gross motor development, walked unsupported 8 yr: Normal mental and fine and gross motor development Required persistent feeding by gastrostomy and had exercise intolerance into adolescence 15 yr: Reported asymptomatic 25 yr: Episode of rhabdomyolysis (serum myoglobin 2X unl, serum CK >4X unl) 27 yr: Motor function, muscle strength at rest, and deep tendon reflexes were normal. Increased serum CK level (>3X unl) 29 yr: No clinical examination was performed, the patient reported being asymptomatic	Mother (R1) has had no clinical signs or symptoms of myopathy, biopsy did not show any signs of mitochondrial myopathy or any other muscle disease

TABLE 1 (Continued)

Family	Patient age at onset	Infantile clinical presentation	Longitudinal follow-up	Family history
4	P6/F 4 y	No signs or symptoms of myopathy in infancy	4 yr: Presented with stumbling gait. 6 yr: Poor balance, complained of leg pain. 10 yr: Experienced muscle fatigue which deteriorated after periods of activity, feeding difficulties, thin stature. Her cognitive skills are assessed as being in the borderline range	P6 and P7 are two out of four children of consanguineous parents. Both parents and the two siblings are healthy and have no signs or symptoms of myopathy. The mother had three miscarriages
	P7/F Birth	Born at term with generalized hypotonia, absence of deep tendon reflexes. Flexion contractures of fingers, adducted thumbs, bilateral clubfeet, bilateral hip dysplasia. Required nasogastric tube feeding because of difficulties in sucking and swallowing. Blood lactate normal	3 mo: Deterioration with respiratory tract infection that required assisted ventilation, which later could be phased out to be used only during sleep. 11 mo: Gastrostomy because of swallowing difficulties. Hypotonia, decreased movement, weak voice during her first year of life. Delayed fine and gross motor development. 2 yr and 3 mo: Normal mental and fine motor development. Generalized hypotonia, more proximally than distally. Can sit but not stand. Soft muscles upon palpation. No deep tendon reflexes. Breathing support during sleep. Weight and length – 3 SD	

Abbreviations: F, female; M, male; mo, month(s); P, patient; unl, upper normal levels; wk, week; yr, years.

was performed. Immunohistochemistry was performed as described previously [10] with antibodies against subunits of the five respiratory chain complexes (complex I: NDUFB8; complex II: SDHB; complex III: UQCRC2; complex IV: MTCO1; complex V: ATPB; as well as the mitochondrial marker VDAC1 (porin); Table S1). In P7, the expression of nesprin-1 was also investigated because of an identified *SYNE1* gene variant (Table S1).

Biochemical analysis including spectrophotometric analysis was performed as previously described [11].

Western blot analysis was performed on proteins extracted from skeletal muscle tissue. Five µg of protein/well was separated on precast 4%–12% Bis-Tris gels (Thermofisher Scientific, Carlsbad, CA, USA) and transferred onto a polyvinylidene difluoride membrane. Antibodies targeted against subunits of the five respiratory chain complexes and VDAC1 were used. For P7, the expression of nesprin-1 was also investigated. For antibodies used, see Table S1. Proteins were detected using the Super Signal West Femto Substrate (Pierce, Rockford, IL, USA) and enhanced chemiluminescent detection (Fujifilm LAS-4000) was used for visualization. Coomassie staining of myosin heavy chain was used as a loading control.

Sanger sequencing was applied for mtDNA analysis in patients and relatives in families 1–3. Whole-genome sequencing was performed in four individuals of family 4 (P6, P7, and both parents). Confirmation analysis was performed by Sanger sequencing in the investigated individuals of family 4.

3 | RESULTS

3.1 | Muscle histopathology and biochemistry

Muscle biopsy was performed in infancy in all patients except P6, who was 9 years (yr) of age at the time of biopsy. In three patients (P1, P2, P5), follow-up biopsies were also carried out. The results from enzyme histochemical, immunohistochemical, ultrastructural, and biochemical analyses are summarized in Table 2. At all occasions, all patients showed mitochondrial myopathy with a variable number of COX-deficient fibers. When analyzed by immunohistochemistry, there was a consistent deficiency of complex I subunit NDUFB8 and complex IV subunit MTCO1 (Figures 2 and 3; Figures S1–S11). The subunit SDHB of complex II was accumulated in accordance with mitochondrial proliferation, as was the mitochondrial membrane protein VDAC1 (porin). There was no deficiency of the subunit UQCRC2 of complex III or subunit ATPB of complex V in any investigated specimens. In addition to mitochondrial alterations, follow-up biopsies in P2 (age 14 yr) and P5 (age 8 yr) revealed unspecific myopathic changes including muscle fiber necrosis, regeneration, and endomysial fibrosis, consistent with a chronic myopathic degenerative process (Figures

TABLE 2 Results from muscle biopsy

Family	Patient	Age at onset	Age at biopsy	Muscle pathology and enzyme analysis				
				Structural changes	Ultrastructural mitochondrial changes	COX⁻ fiber (%)	Immunohistochemical investigation	Enzyme activities
1	P1/M	1 mo	4 mo	Fiber size variability, lipid accumulation, RRFs Figure S1	Large subsarcolemmal and intermyofibrillar collections of giant mito. with circular and tubular cristae, lipid accumulation Figure 4A,B	60	nd	CI: 1200 (ref. 4500–8600) CIV: 1.9 (ref. 6.1–15)
			18 yr	Mito proliferation, some RRF Figure 2C; Figure S2	Subsarcolemmal accumulation of partly giant mito. with irregular cristae and paracrystalline inclusions Figure 4C,D	40	NDUFB8 reduced (60%[a]) MTCO1 reduced (partial) SDHB increased Figure 2C	nd
2	P2/M	1 mo	2 mo	Fiber size variability, lipid accumulation, RRFs Figure S3	Large intermyofibrillar accumulation of giant mito. with abnormal cristae, lipid accumulation Figure 4E,F	95	nd	CI: 0 (udl) (ref. 4500–8600) CIV: 0.9 (ref. 6.1–15)
			5 yr	Slight fiber size variability, some internalized nuclei, some fibers with mito. proliferation Figure S4	Subsarcolemmal accumulation of elongated mito. with dense matrix Figure 4G,H	5	nd	CI: 4100 (ref. 4500–8600) CIV: 9.1 (ref. 6.1–15)
			14 yr	Marked fiber size variability, internalized nuclei, fiber splitting, increased connective tissue, occasional muscle fiber necrosis, mito. proliferation Figure S5	nd	60	NDUFB8 reduced (80%[a]) MTCO1 reduced (partial) SDHB increased	CI: 3200 (ref. 4500–8600) CIV: 7 (6.1–15)
	P3/M	1 mo	1 mo	Fiber size variability, lipid accumulation, RRFs Figure S6	nd	80	nd	CI: 1150 (ref. 4500–8600) CIV: 0.54 (ref. 6.1–15)
	P4/F	2 mo	4 mo	Fiber size variability, lipid accumulation, RRFs Figure S7	Large subsarcolemmal and intermyofibrillar collections of giant mito. with circular and tubular cristae, lipid accumulation Figure 5A,B	75	NDUFB8 reduced (80%[a]) MTCO1 reduced (50%[a]) SDHB increased	CI: 925 (ref. 4500–8600) CIV: 1.1 (ref. 6.1–15)

(Continues)

TABLE 2 (Continued)

Family	Patient	Age at onset	Age at biopsy	Muscle pathology and enzyme analysis				
				Structural changes	Ultrastructural mitochondrial changes	COX⁻ fiber (%)	Immunohistochemical investigation	Enzyme activities
3	P5/F	3 wk	1 mo	Fiber size variability, lipid accumulation, RRFs, Figure 2A; Figure S8	Large subsarcolemmal and intermyofibrillar collections of giant mito. with abnormal cristae and enlarged, elongated mito. with dense matrix, lipid accumulation Figure 5C,D	80	NDUFB8 reduced (95%[a]) MTCO1 reduced (60%[a]) SDHB increased Figure 2A	CI: 930 (ref. 4500–8600) CIV: 0.22 (ref. 6.1–15)
			8 yr	Fiber size variability, increased connective tissue, internalized nuclei, fiber necrosis and regeneration, mito. proliferation Figure 2B; Figure S9	nd	20	NDUFB8 reduced (severe, regional) MTCO1 reduced (partial) SDHB increased Figure 2B	CI: 6140 (ref. 4500–8600) CIV: 14 (ref. 6.1–15)
4	P6/F	4 yr	9 yr	Fiber size variability, some fibers with lipid accumulation, mito. proliferation, some RRFs Figure 3B; Figure S10	Subsarcolemmal and intermyofibrillar collections of enlarged, partly elongated, mito. with single or multiple inclusions Figure 5E,F	5	NDUFB8 reduced (moderate, regional, 10%[a]) MTCO1 reduced (mild, regional) SDHB increased Figure 3B	nd
	P7/F	Birth	1 mo	Pronounced fiber size variability, increased connective tissue, some fibers with internal nuclei, lipid accumulation, nesprin-1 absent from nuclear membranes Figures 3A and 7; Figure S11	Intermyofibrillar collection of elongated mito. with dense matrix, lipid accumulation Figure 5G,H	15	NDUFB8 reduced (60%[a]) MTCO1 reduced (10%[a]) SDHB increased Figure 3A	nd

Note: Enzyme activities: CI = nmol/min × mg protein; CIV = k/mg protein; k = rate constant.

Abbreviations: CI, complex I; CIV, complex IV; COX⁻, COX-deficient fibers in COX/SDH staining; F, female; M, male; mo, month; mito., mitochondria; nd, no data; RRF, ragged-red fiber; udl, under detection limit; wk, weak; yr, year.

[a]Proportion of fibers with complete lack of immunoreactivity.
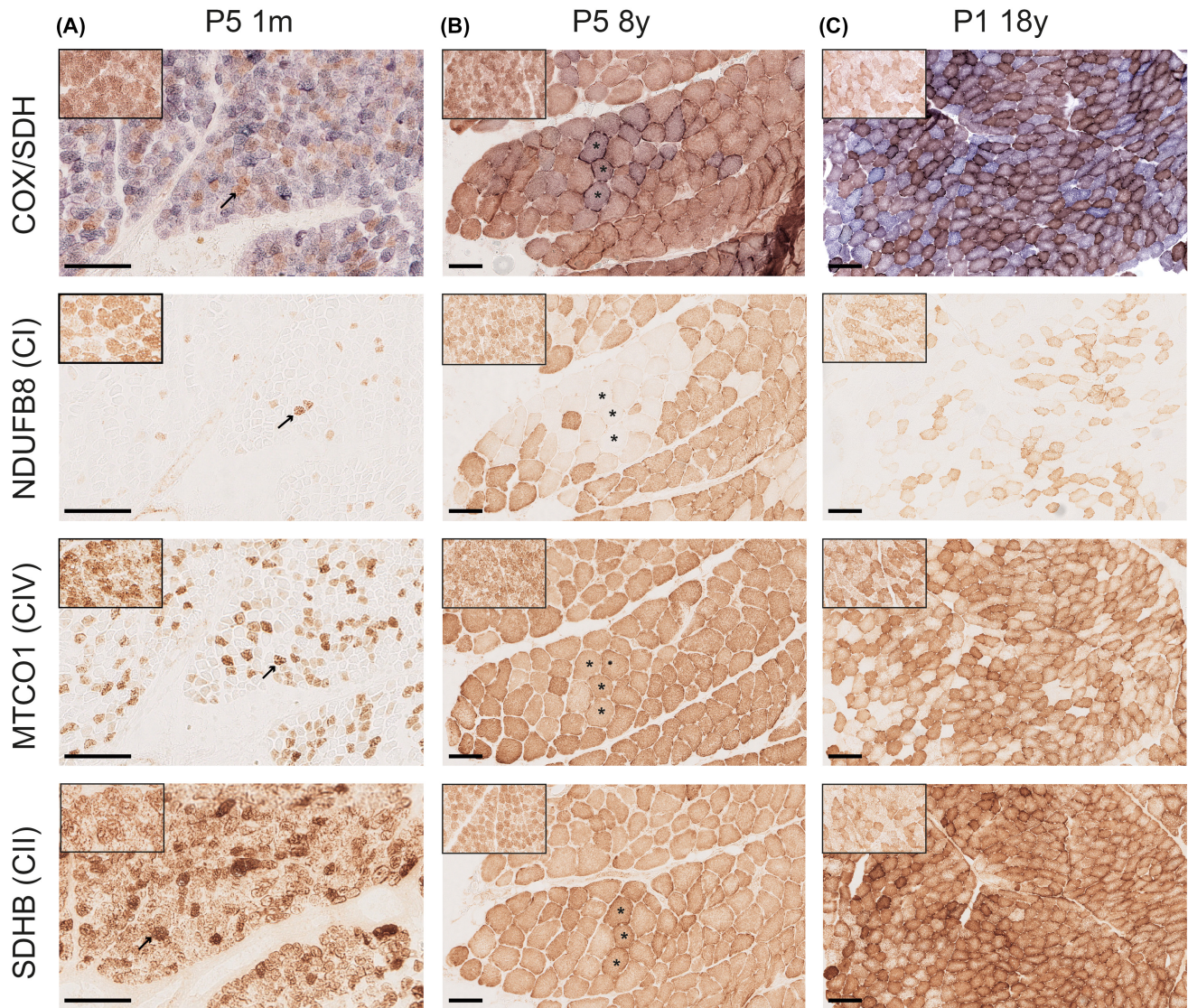
FIGURE 2 Serial sections of skeletal muscle of P5 and P1 at different ages. COX/SDH enzyme histochemistry with fiber lacking COX activity staining blue. Immunohistochemistry was used to visualize NDUFB8 (complex I), MTCO1 (complex IV), and SDHB (complex II). (A) P5 at 1 mo of age. A majority of the fiber show COX deficiency. A marked decrease of NDUFB8 and MTCO1 is seen, although the lack of MTCO1 is not as pronounced as the lack of NDUFB8. Some myofibers show high expression of SDHB. Identical fibers are marked with arrows. (B) P5 at 8 yr of age. A few fiber show partial COX deficiency. About 25% of the fiber lack NDUFB8 staining. These fibers show a regional distribution, rather than an even distribution. Some cells reveal a decrease in MTCO1 staining, but there is not a complete absence as seen at 1 mo of age. Occasional fibers show hyper-reactivity of SDHB. Identical fibers are marked with asterisks. (C) P1 at 18 yr of age. Numerous fibers show COX deficiency. A majority of the fibers lacks NDUFB8. Some fibers demonstrate decreased MTCO1 expression, only a few scattered fibers completely lack MTCO1. The fibers with abolished MTCO1 expression also completely lack NDUFB8. Some fibers show hyper-reactivity of SDHB. Insets show staining of a control aged 1.5 yr. Scale bars measure 100 μm

S5 and S9). Follow-up biopsies in P1 (age 18 yr), P2 (age 5 yr), and P6 (age 9 yr) showed mainly mitochondrial alterations with enzyme deficiency and mitochondrial proliferation (Figures 2B,C and 3B; Figures S2, S4, and S10). P7 at age 1 month (mo) showed marked variability of fiber size with markedly increased interstitial connective tissue in addition the frequent COX-deficient fibers and immunohistochemical deficiency of complex I and complex IV (Figures 3A and 7A–C; Figure S11). In P2, a type 2 fiber predominance was seen at 5 yr of age, whereas there was normal fiber type distribution nine years later at age 14. In contrast, the follow-up biopsy in

P5 demonstrated solely type 1 fibers. The follow-up biopsy in P1 demonstrated normal fiber type distribution.

Biochemical analyses of the respiratory chain enzyme complexes revealed profound combined complex I and IV deficiency in all examined infant patients and milder defects at follow-up (Table 2).

3.2 | Ultrastructural analysis

Electron microscopic analysis of mitochondria in infant P1, 2, 4, and 5 biopsies demonstrated intermyofibrillar and
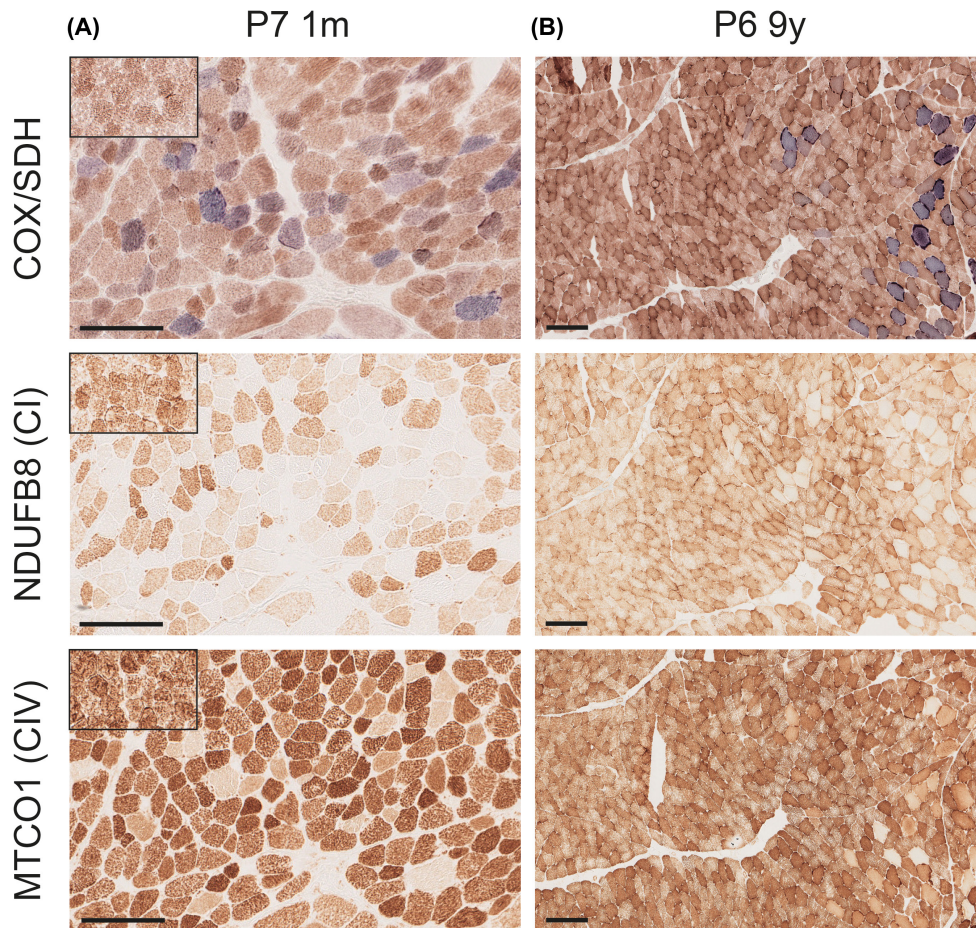
FIGURE 3 Serial sections of skeletal muscle of affected individuals in Family 4 (P7 and P6). COX/SDH enzyme histochemistry with fibers lacking COX activity staining blue. Immunohistochemistry was used to visualize NDUFB8 (complex I) and MTCO1 (complex IV). (A) P7 at 1 mo of age. Numerous fibers show COX deficiency. A majority of the fibers lack NDUFB8 staining and some fibers show reduced expression of MTCO1. Only a few scattered fibers completely lack MTCO1 expression. Insets show staining of an age-matched control. (B) P6 at 9 yr of age. Numerous fibers show COX deficiency. Numerous but not a majority of the fibers completely lack NDUFB8 expression with regional differences and some fibers show a decreased expression. Scattered fibers show a reduced of MTCO1 expression. Scale bars measure 100 μm

subsarcolemmal accumulation of enlarged, frequently giant mitochondria with circular and tubular cristae in addition marked increase in fat (Figures 4A,B,E,F and 5A–D). In follow-up investigations of P1 at age 18 yr (Figure 4C,D), and P2 at 5 yr (Figure 4G,H), and in P6 at age 9 yr (Figure 5E,F) the mitochondrial changes were seen as subsarcolemmal and partly intermyofibrillar accumulation of mitochondria with paracrystalline and other inclusions and frequently elongated mitochondria with dense matrix. P7 showed in addition to abnormal elongated mitochondria with dense matrix (Figure 5G,H), numerous atrophic fibers, myofibrillar disorganization and multilobulated nuclei.

3.3 | Immunoblotting

To analyze possible effects of the m.14674T>C variant on protein expression of the individual respiratory chain complexes, protein expression in homogenates of skeletal muscle from all patient biopsies, from the mother of P5

(R1), and two healthy controls (C1 and C2, both one year of age) was determined (Figure 6). This revealed a severe reduction of NDUFB8 in the patients' muscle biopsy specimens in infancy. Results from analysis of an additional subunit of complex I, NDUFS3, in family 4 showed a similar pattern as NDUFB8 (Figure S12). Expression of MTCO1 was also downregulated, but not to the same extent as NDUFB8. These results are in agreement with the results from immunohistochemical analyses.

In follow-up biopsies, when the patients had recovered (P2 5 yr and P5 8 yr), as well as in the healthy mother of P5 (R1), the expression levels of NDUFB8 and MTCO1 were normal. However, the expressions of both NDUFB8 and MTCO1 were decreased in P2 at 14 yr of age, when his muscle function had deteriorated. This finding is in concordance with histology results showing an increase in COX-deficient fibers. In the follow-up biopsy of P1 at 18 yr of age, the expression of NDUFB8 was reduced, while the expression of MTCO1 was normal. Some of the patients showed an
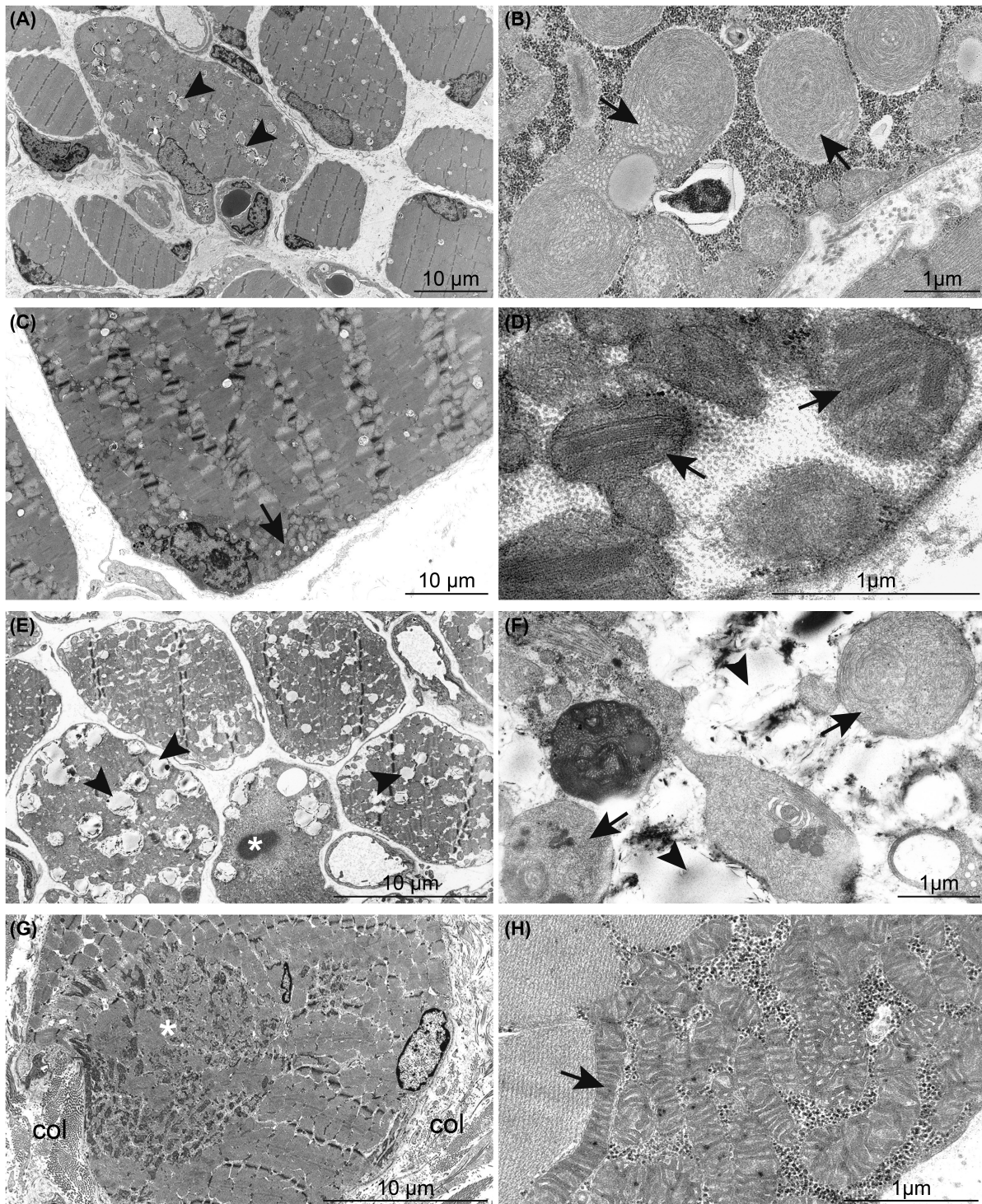
FIGURE 4 Electron micrographs of skeletal muscle from P1 and P2. (A and B) P1 at age 4 mo showing increased fiber size variability and large fat droplets (arrowheads) in some fibers. Collections of giant mitochondria with circular and tubular cristae are present in many fibers (arrows). (C and D) P1 at age 18 yr showing subsarcolemmal collections of mitochondria with paracrystalline inclusions (arrows). (E and F) P2 at age 2 mo showing an increased variability in fiber size and large fat droplets (arrowheads) in several fibers. Collections of giant mitochondria with tubular and circular cristae are present in many fibers (arrows). There is also a cytoplasmic body present in one fiber (asterisk). (G and H) P2 at age 5 yr showing subsarcolemmal collections of mitochondria with elongated shape and dense matrix (arrow). There is also a core structure in a fiber (asterisk) and increased interstitial collagen (col)

increase in the expression of SDHB (P2 at 2 mo of age, P3, P4, and both biopsies of P5 and P1), consistent with muscle biopsy findings of mitochondrial proliferation (Figure 6). These biopsies also showed an increase in VDAC1 expression, albeit not as immense as the increase in SDHB expression, compared to controls.
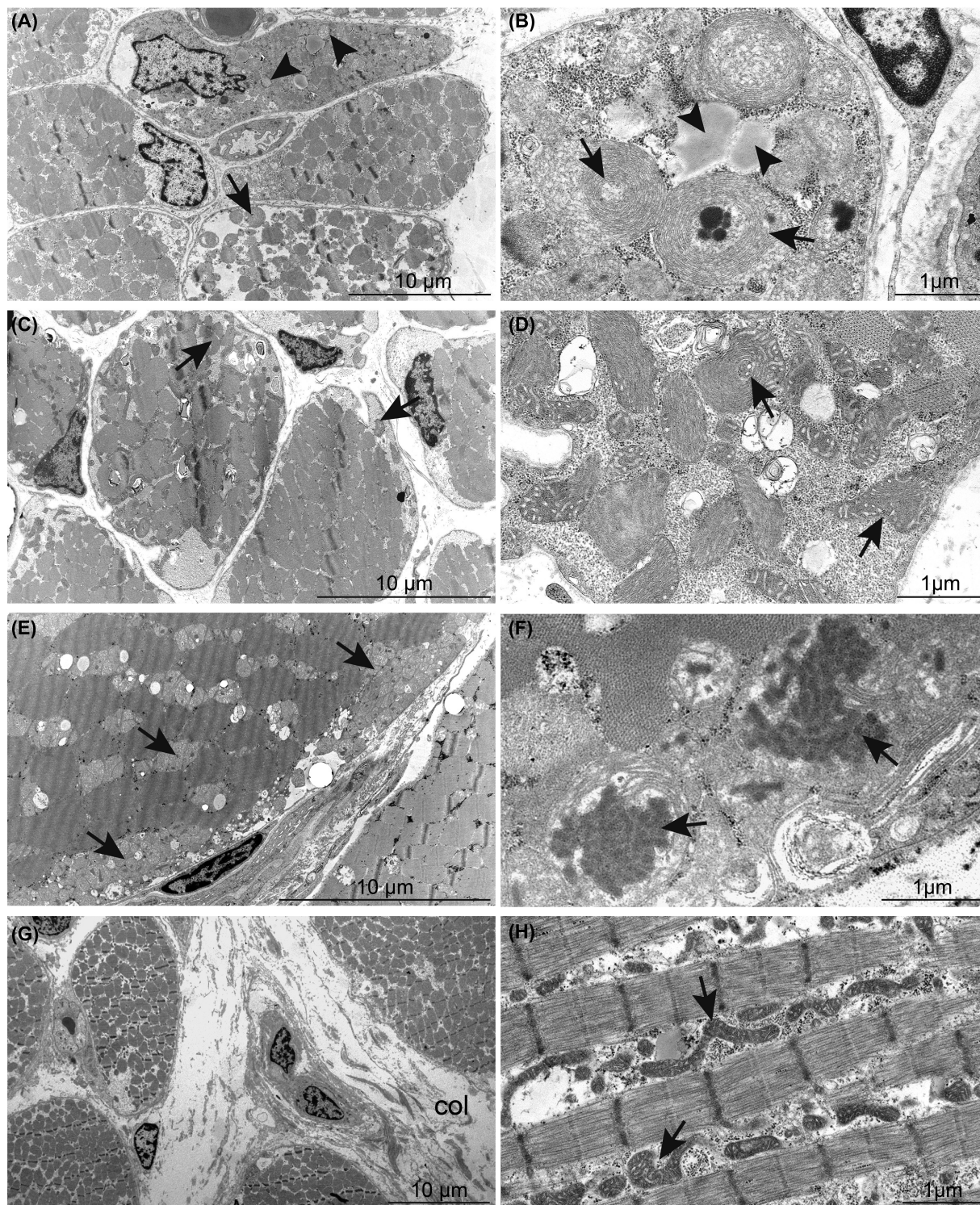
FIGURE 5 Electron micrographs of skeletal muscle from P4, P5, P6 and P7. (A and B) P4 at age 4 mo showing collections of giant mitochondria with circular and tubular cristae (arrows). (C and D) P5 at age 1 mo showing muscle fibers with subsarcolemmal accumulation of glycogen and collections of large mitochondria (arrows). The mitochondria show circular and tubular cristae with dense matrix. (E and F) P6 at age 9 yr showing subsarcolemmal and intermyofibrillar collections of large mitochondria multiple inclusions (arrows). (G and H) P7 at age 1 mo showing increased fiber size variability and increased interstitial collagen (col). Some fibers show increased amounts of elongated intermyofibrillar mitochondria with dense matrix (arrows)

To determine whether the nonsense variant in *SYNE1* affected protein translation, protein levels in skeletal muscle of P7 as well as two age-matched controls were examined using an antibody, MANNES1E, directed against both the nesprin-1 giant isoform as well as the short nesprin-1α2 isoform (Table S1). The
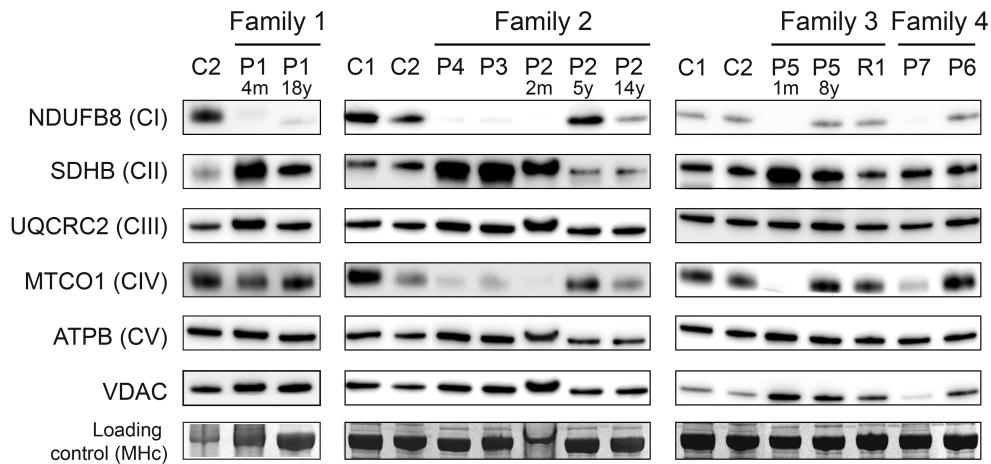
FIGURE 6 Immunoblotting shows decreased levels of the complex I subunit NDUFB8 and the complex IV subunit MTCO1 in patients' muscle biopsy specimens in infancy. In follow-up biopsies, when the patients showed clinical improvement (P2 5y and P5 8y), as well as in the healthy mother of P5 (R1), the expression levels of NDUFB8 and MTCO1 were normal. The expression of both NDUFB8 and MTCO1 was decreased in P2 at age 14 yr, while only NDUFB8 expression was decreased in P1 at 18 yr of age. Coomassie staining of the myosin heavy-chain band (MHc) serves as loading control. C, control, P, patient, R, relative
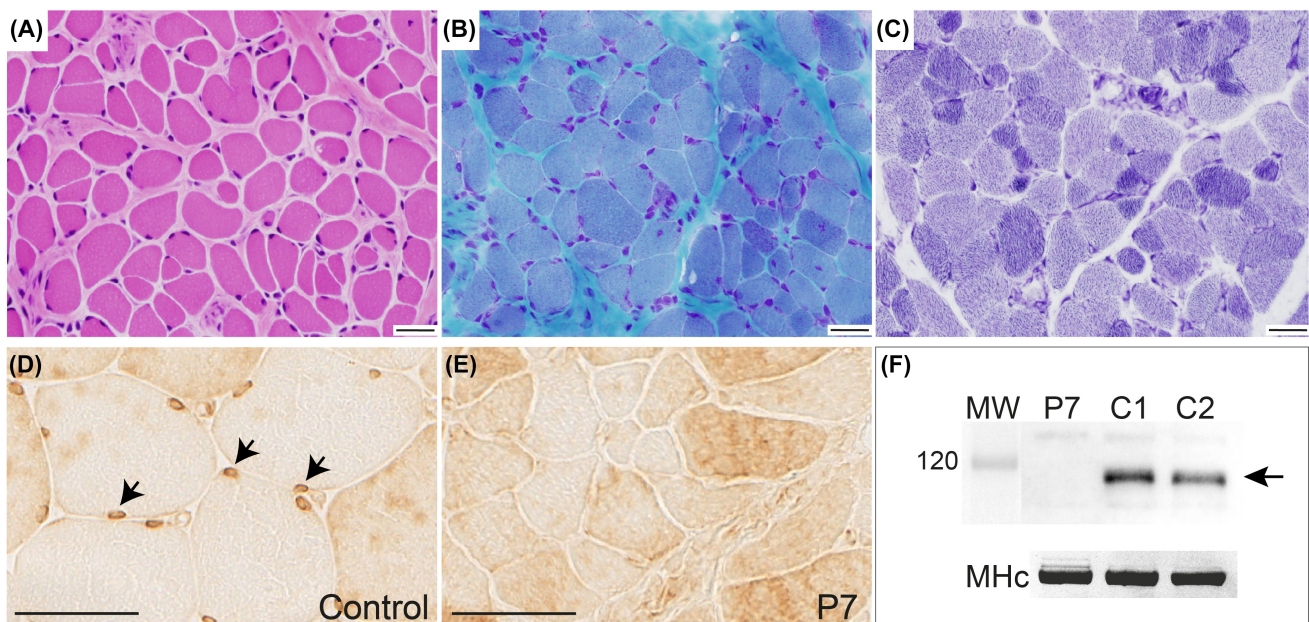
FIGURE 7 Muscle pathology and Nesprin expression in P7. (A–C) Quadriceps muscle at 1 mo of age. There is marked variability of fiber size (range: 5–40 μm) and marked increase in connective tissue (A, H&E; B, Gomori trichrome; C, NADH-tetrazolium reductase; Scale bars measure 40 μm). (D and E) Immunohistochemistry using MANNES1A that recognizes the C-terminal region of nesprin-1-giant as well as nesprin-1-α2, the short isoform of nesprin-1, shows distinct staining of the nuclear rim (arrowheads) in an adult biopsy without signs of muscle disease, serving as a control (D). No such staining could be detected in P7 (E), (scale bars measure 50 μm). (F) Western blotting using MANNES1E showing that the expression of nesprin-1 was completely abolished in P7. Coomassie staining of the myosin heavy-chain band (MHc) serves as loading control

protein expression of nesprin-1 in P7 was entirely abolished (Figure 7F). In agreement with this finding, immunohistochemistry with an antibody against nesprin-1 (MANNES1A) demonstrated absence of the normal distinct staining of the nuclear membrane (Figure 7D,E).

3.4 | Genetic analysis

P1–P3 and P5 have previously been reported to carry the homoplasmic m.14674T>C variant in *MT-TE* [1, 6]. In P4, sequencing of all mitochondrial tRNA genes revealed the same alteration. The mothers of P1, P2, P3,

P4, and P5 carried the homoplasmic m.14674T>C variant, but it was absent in the father of P5 (Figure 1).

Whole-genome sequencing was conducted in four family members of family 4, including P6, P7, and their parents, in reference to the clinical findings of myopathy and arthrogryposis and mitochondrial changes on muscle biopsy in P7 and the mitochondrial myopathy in P6. In P7, two pathogenic variants were found, one homozygous variant in *SYNE1* (c.25448G>A, NM_033071.3) resulting in a premature stop codon p.Trp8483* not reported in the Genome Aggregation Database (gnomAD), as well as the previously reported m.14674T>C variant. The parents were heterozygous for the *SYNE1* variant and both of them were homoplasmic for the m.14674T>C variant. P6 carried the m.14674T>C variant in tRNA^{Glu} (Figure 1). No homozygous- or compound heterozygous-predicted pathogenic variants were detected in *EARS2*, *TRMU*, *QRSL1*, *GOT2*, *GLS*, or *MSS51*, genes known to interact with mt-tRNA^{Glu}. Damaging variants in such genes have been suggested to be a prerequisite for development of reversible infantile respiratory chain deficiency in carriers of the homoplasmic m.14674T>C variant [7]. Further filtering for variants in nuclear genes interacting with mt-tRNA^{Glu} predicted as deleterious identified one heterozygous variant in *MTO1* (c.1933C>A, NM_012123.4; p.Arg645Ser) in P7 and her mother.

4 | DISCUSSION

Reversible infantile respiratory chain deficiency was first described in 1981 [5]. The disease-causing m.14674T>C variant was identified in 17 patients by Horvath and co-workers in 2009 [1], and two other cohorts were published shortly thereafter [2, 3]. In the Japanese cohort [2], eight patients were investigated, and the same variant was identified in six of the patients. Interestingly, two patients carried a novel homoplasmic m.14674T>G variant, with the same clinical phenotypes as the patients with the m.14674T>C variant. The clinical presentation of the patients in these three papers has been summarized by Boczonadi et al. [12] and includes muscle weakness, hypotonia, and feeding difficulties in almost all patients, whereas mechanical ventilation was required in about 1/3 of the patients. The natural history of the condition is not well known. Uusimaa and co-workers presented longitudinal follow-up data from early infancy into adulthood of six patients with the m.14674T>C variant, suggesting that even though the profound muscle weakness seen at presentation improved, subtle symptoms may persist. These symptoms included fatigue, myalgia, and facial weakness [3].

All patients in our cohort showed improvement following the acute episode in infancy, except P6, who did not show symptoms in infancy, but was found to have myopathic symptoms at 4 yr of age. P2, who presented in infancy with muscle weakness and hypotonia, did initially improve, and at 5 yr of age, he had recovered clinically and according to the muscle biopsy findings. However, at age 14 yr, he had deteriorated clinically and according to muscle biopsy findings. At the last follow-up at age 32 yr, the patient demonstrated worsening of symptoms with exercise intolerance, myalgia, and decline in ambulation and serum CK was increased. P1 experienced, at age 18 yr, exercise intolerance in accordance with the mitochondrial myopathy with 50% COX deficient fiber. These findings from our follow-up investigations illustrate that disease associated with the m.14674T>C variant is variable and not always reversible but instead frequently progressive despite an initial phase of recovery in patients with infantile onset. It can also manifest as a slowly progressive myopathy without an infantile episode of muscle weakness. Uusimaa and co-workers suggested that the clinical recovery of the patients in their cohort was due to a loss of a subpopulation of COX-negative muscle fibers, which was supported by type 2 fiber predominance in a follow-up biopsy after improvement of symptoms [3]. In our cohort, four follow-up biopsies were performed, but no such conclusions regarding an effect of change in fiber-type composition could be drawn from the results in our studies.

The light microscopical morphological muscle biopsy findings were very similar in all infantile cases with profound COX deficiency, mitochondrial proliferation with ragged red fibers, fiber caliber variation, and abnormal lipid accumulation. The only exception was patient 7 who, in addition, suffered from a congenital myopathy due to nesprin-1 deficiency. The mitochondrial ultrastructural changes were also uniform with large mitochondria with circular and tubular cristae. Later in childhood, in adolescence and adulthood the characteristic ultrastructural changes of infancy were no longer present but instead abnormal mitochondria were characterized by elongated shape, dense matrix and inclusions, some of which were the typical paracrystalline inclusions seen in adults with mitochondrial myopathy due to mtDNA mutations. These inclusions are not typically seen in infancy and our longitudinal study clearly shows that the type of mitochondrial structural abnormalities is age-related. Our follow-up study also demonstrates that the disease associated with m.14674T>C variant frequently persists into adulthood as a mitochondrial myopathy, which in some cases shows dystrophic features with muscle fiber necrosis, regeneration, and fibrosis. These changes may underlie the progressive clinical features seen in some cases.

In P7, who also carried the homozygous *SYNE1* stop mutation causing nesprin-1 deficiency and a congenital myopathy, the morphological changes were very different from the other infants. Her biopsy at age 1 mo showed marked fiber size variability and increased connective tissue, indicating an in utero onset of a degenerative muscle disorder. In addition, she had frequent COX-deficient fibers, which indicated an additional mitochondrial disease. As we could demonstrate a combined complex I and IV deficiency, the apparent explanation for the

mitochondrial enzyme deficiency was the m.14674T>C variant. Interestingly she did not show the same ultrastructural mitochondrial alterations as the other infants but changes that were more similar to those seen in follow-up biopsies in the other cases. Another difference was the reduced expression of VDAC (porin), a mitochondrial membrane protein. This reduced expression was not explained by a reduced number of mitochondria as the SDH staining and western blot of SDHB, was like the other cases. It may be speculated that the nesprin-1 deficiency somehow altered the mitochondrial membrane structure.

An important finding in this study is the deficiency of the complex I subunit NDUFB8 in our patients, as demonstrated by both immunohistochemistry and western blot. A combined enzyme deficiency of complex I and complex IV activities have previously been shown [1–3], but complex I expression has not previously been studied immunohistochemically in patients with reversible infantile respiratory chain deficiency. The investigated patients showed a more pronounced NDUFB8-deficiency than MTCO1-deficiency, indicating a greater disturbance in complex I assembly than in complex IV. Furthermore, the follow-up biopsies of P1 and P5 showed greater reversibility in MTCO1 expression than in NDUFB8 expression, and there was a remaining regional deficiency of mainly NDUFB8 as revealed by immunohistochemistry. Moreover, the deterioration of symptoms in P2 coincides with the decrease in expression of NDUFB8 rather than MTCO1 expression, as demonstrated by immunohistochemistry and western blot analyses. A combined, but predominant complex I, respiratory chain deficiency is known to be caused by some variants in mt-tRNA genes, particularly *MT-TL1* (mt-tRNA$^{Leu(UUR)}$) [13, 14], but the mechanisms by which these variants affect mainly complex I activity is unclear. One explanation could be that complex I has the highest number of subunits encoded by the mitochondrial genome, therefore making it more vulnerable when there are disease-causing variants in affecting mt-tRNA genes. Leu residues are especially prevalent in complex I, and the number of Glu residues is also much higher than in the other complexes (Table S2).

As described previously, the penetrance of the disease is incomplete [1], with many homoplasmic carriers never becoming affected. In the gnomAD, consisting of 56429 individuals, two homoplasmic and three heteroplasmic carriers of the m.14674T>C variant were found. The m.14674T>G variant was not present in any of the individuals. In our cohort, we have detailed information on four of the parents, of which none have had any signs or symptoms of myopathy. Incomplete penetrance is also seen for other homoplasmic disease-causing mtDNA variants such as in Leber's hereditary optic neuropathy (LHON), where it has been established that 50% of males and only 10% of females carrying a homoplasmic disease-causing variant develop clinical characteristics of the disease. The cause of the incomplete penetrance in

LHON is still poorly understood, but it is believed to be an interaction between the primary genetic defect, environmental triggers, such as smoking, and genetic modifying factors such as mtDNA haplotype, mtDNA copy number, and nuclear modifiers [15].

A recent study [7] proposed that reversible infantile respiratory chain deficiency is inherited in a digenic manner, suggesting that besides the mtDNA variant, an additional heterozygous variant in a nuclear gene interacting with mt-tRNA^{Glu} modifies the phenotypic outcome of the m.14674T>C variant. In that study, heterozygous genetic variants were found in several genes, with *EARS2* and *TRMU* being the most common. In two affected individuals, no additional variant considered to be involved in the pathogenesis was found. One patient inherited both the homoplasmic m.14674T>C variant and an *EARS2* variant from her healthy mother. The latter was not reported with any history of muscle problems during early development or later in life. In our study, we thoroughly investigated family 4 genetically. In this family, the parents of the two affected individuals are first cousins, both homoplasmic for the m.14674T>C variant. We did not find any homozygous or heterozygous variants predicted as pathogenic in *EARS2*, *TRMU*, *QRSL1*, *GOT2*, *GLS*, or *MSS51* in this family and no *de novo* variants of interest were identified in the affected children. One heterozygous variant was identified in *MTO1*, a gene involved in mt-tRNA^{Glu} modification [16], in both P7 and her mother, but not in the affected sibling P6. This variant has previously been reported as pathogenic, causing brain malformations in an autosomal recessive manner [17]. As the *MTO1*-variant identified in family 4 does not co-segregate with the disease, it is unlikely to function as a genetic modifier. P3 and P4 are half siblings and they inherited the homoplasmic m.14674T>C variant from their mother, who had no history of muscle weakness. It seems unlikely, albeit not utterly excluded, that they inherited a pathogenic modifying genetic variant for they had different fathers. Thus, the inheritance pattern in family 2 and family 4, and the detailed genetic analysis in family 4 do not support the concept of digenic inheritance of reversible infantile respiratory chain deficiency.

P7 in our cohort, who presented with muscle weakness, adducted thumbs, flexion contractures of fingers, and bilateral clubfeet was found to carry, in addition to the m.14674T>C variant, a novel homozygous variant c.25448G>A in *SYNE1*, causing a premature stop codon, p.Trp8483*. *SYNE1*, the synaptic nuclear envelope protein-1 gene, encodes nesprin-1, a protein involved in the positioning of the nucleus in skeletal muscle cells [18]. To date, five patients with arthrogryposis carrying variants in *SYNE1* have been identified [19–21]. Protein expression using antibodies directed against the common C-terminal region of nesprin-1-giant as well as nesprin-1-α2, the short isoform of nesprin-1,

indicated that the protein expression of nesprin-1 in P7 was completely abolished. Muscle morphology has only been described in one patient with arthrogryposis and a *SYNE1* variant. That muscle biopsy revealed nuclear changes in form of multiple invaginations of the nuclear membrane, multilobulated, honeycombed nuclei, and a variation in size of muscle fibers [20]. These findings corroborate with muscle biopsy findings in P7 in our study, which demonstrated fiber size variability and fibrosis. Ultrastructural analysis displayed nuclear membrane invaginations and multilobulated nuclei, findings which may be associated with the absence of normal nesprin-1. Our study confirms that variants in *SYNE1* cause autosomal recessive arthrogryposis and that nesprin-1 variants should be considered as a possible cause in patients presenting with muscle weakness and contractures in infancy.

This study is based on patients who were infants when they came to our attention and several of them are now adults. In most cases they received a genetic diagnosis after sequencing of the mitochondrial DNA after investigation of the muscle biopsy showing a mitochondrial myopathy. Nowadays it is common to start the genetic investigation by next generation sequencing (NGS) applying whole exome or genome sequencing (WES/WGS) even before muscle biopsy [22]. Applying NGS as in the case of family 4, with filtering against genes known to cause congenital myopathy, disclosed the *SYNE1* variant explaining the clinical phenotype at birth. However, muscle biopsy was essential in this case because it clearly demonstrated a mitochondrial enzyme deficiency, which led to identification of the m.14674T>C variant, which in turn explained the clinical deterioration at 3 mo of age. Double trouble in this patient was identified by careful genetic analysis and muscle biopsy, which was necessary for evaluating the clinical condition and treatment. In the case of the m.14674T>C variant it is usually homoplasmic and therefore possible to identify in blood DNA but many pathogenic mtDNA variants are heteroplasmic and may be present only in affected tissues [23, 24].

To our knowledge, this is the first study investigating the expression of the individual respiratory chain complexes by immunohistochemistry and western blot in a cohort of patients with reversible infantile respiratory chain deficiency. Our findings indicate that the respiratory chain complex I is mainly affected. This is a descriptive study, and we can therefore not draw any definite pathophysiological conclusions about the mechanism behind the defective assembly of complex I. Still, it sheds new light on the involvement of individual complexes of the respiratory chain in reversible infantile respiratory chain deficiency. The reversibility of the disease remains unexplained and it has been proposed that unknown nuclear factor(s) relating to the control of the amount of tRNA^{Glu} may be key factors in mechanisms of recovery [2]. Further studies are needed to explore these mechanisms. Our study also demonstrates that not all features of the disorder are entirely transient, that the disease may be progressive, and that myopathy can develop without an infantile episode with hypotonia and weakness.

CONFLICT OF INTEREST
The authors declare that they have no conflict of interest.

AUTHOR CONTRIBUTIONS
Sara Roos and Anders Oldfors designed the study, analyzed the data, drafted and revised the manuscript. Carola Hedberg-Oldfors analyzed the genetic data, drafted and revised the manuscript. Kittichate Visuttijai performed western blotting experiments and contributed to the final version of the manuscript. Gittan Kollberg was involved in acquisition of the biochemical data and contributed to the final version of the manuscript. My Stein, Ólöf Elíasdóttir, and Christopher Lindberg were involved in acquisition of the clinical data and contributed to the final version of the manuscript. Niklas Darin was involved in acquisition of the clinical data, drafted and revised the manuscript.

ETHICAL APPROVAL
All protocols were approved by the Regional Ethical Review Board in Gothenburg. All the material in this study was obtained for diagnostic purposes and permitted for scientific use with informed consent.

DATA AVAILABILITY STATEMENT
The data that support the findings of this study are available from the corresponding author upon reasonable request.

ORCID
Sara Roos https://orcid.org/0000-0002-2165-2345
Kittichate Visuttijai https://orcid.org/0000-0002-4800-8533

REFERENCES
1. Horvath R, Kemp JP, Tuppen HA, Hudson G, Oldfors A, Marie SK, et al. Molecular basis of infantile reversible cytochrome c oxidase deficiency myopathy. Brain. 2009;132:3165–74.
2. Mimaki M, Hatakeyama H, Komaki H, Yokoyama M, Arai H, Kirino Y, et al. Reversible infantile respiratory chain deficiency: a clinical and molecular study. Ann Neurol. 2010;68:845–54.
3. Uusimaa J, Jungbluth H, Fratter C, Crisponi G, Feng L, Zeviani M, et al. Reversible infantile respiratory chain deficiency is a

unique, genetically heterogenous mitochondrial disease. J Med Genet. 2011;48:660–8.

4. Tritschler HJ, Bonilla E, Lombes A, Andreetta F, Servidei S, Schneyder B, et al. Differential diagnosis of fatal and benign cytochrome c oxidase-deficient myopathies of infancy: an immunohistochemical approach. Neurology. 1991;41:300–5.

5. DiMauro S, Nicholson JF, Hays AP, Eastwood AB, Koenigsberger R, DeVivo DC. Benign infantile mitochondrial myopathy due to reversible cytochrome c oxidase deficiency. Trans Am Neurol Assoc. 1981;106:205–7.

6. Houshmand M, Larsson NG, Holme E, Oldfors A, Tulinius MH, Andersen O. Automatic sequencing of mitochondrial tRNA genes in patients with mitochondrial encephalomyopathy. Biochim Biophys Acta. 1994;1226:49–55.

7. Hathazi D, Griffin H, Jennings MJ, Giunta M, Powell C, Pearce SF, et al. Metabolic shift underlies recovery in reversible infantile respiratory chain deficiency. EMBO J. 2020;39:e105364.

8. Oldfors A, Sommerland H, Holme E, Tulinius M, Kristiansson B. Cytochrome c oxidase deficiency in infancy. Acta Neuropathol. 1989;77:267–75.

9. Dubowitz V, Sewry CA, Oldfors A, eds. Muscle biopsy: a practical approach, 4th ed. Philadelphia, PA: Saunders Elsevier; 2013:1–592.

10. Gurgel-Giannetti J, Lynch DS, Paiva ARB, Lucato LT, Yamamoto G, Thomsen C, et al. A novel complex neurological phenotype due to a homozygous mutation in FDX2. Brain. 2018;141:2289–98.

11. Jennions E, Hedberg-Oldfors C, Berglund AK, Kollberg G, Tornhage CJ, Eklund EA, et al. TANGO2 deficiency as a cause of neurodevelopmental delay with indirect effects on mitochondrial energy metabolism. J Inherit Metab Dis. 2019;42:898–908.

12. Boczonadi V, Bansagi B, Horvath R. Reversible infantile mitochondrial diseases. J Inherit Metab Dis. 2015;38:427–35.

13. Swalwell H, Kirby DM, Blakely EL, Mitchell A, Salemi R, Sugiana C, et al. Respiratory chain complex I deficiency caused by mitochondrial DNA mutations. Eur J Hum Genet. 2011;19:769–75.

14. Haack TB, Madignier F, Herzer M, Lamantea E, Danhauser K, Invernizzi F, et al. Mutation screening of 75 candidate genes in 152 complex I deficiency cases identifies pathogenic variants in 16 genes including NDUFB9. J Med Genet. 2012;49:83–9.

15. Caporali L, Maresca A, Capristo M, Del Dotto V, Tagliavini F, Valentino ML, et al. Incomplete penetrance in mitochondrial optic neuropathies. Mitochondrion. 2017;36:130–7.

16. Wang X, Yan Q, Guan MX. Combination of the loss of cmnm5U34 with the lack of s2U34 modifications of tRNALys, tRNAGlu, and tRNAGln altered mitochondrial biogenesis and respiration. J Mol Biol. 2010;395:1038–48.

17. Karaca E, Harel T, Pehlivan D, Jhangiani SN, Gambin T, Coban Akdemir Z, et al. Genes that affect brain structure and function identified by rare variant analyses of mendelian neurologic disease. Neuron. 2015;88:499–513.

18. Zhang J, Felder A, Liu Y, Guo LT, Lange S, Dalton ND, et al. Nesprin 1 is critical for nuclear positioning and anchorage. Hum Mol Genet. 2010;19:329–41.

19. Attali R, Warwar N, Israel A, Gurt I, McNally E, Puckelwartz M, et al. Mutation of SYNE-1, encoding an essential component of the nuclear lamina, is responsible for autosomal recessive arthrogryposis. Hum Mol Genet. 2009;18:3462–9.

20. Baumann M, Steichen-Gersdorf E, Krabichler B, Petersen BS, Weber U, Schmidt WM, et al. Homozygous SYNE1 mutation causes congenital onset of muscular weakness with distal arthrogryposis: a genotype-phenotype correlation. Eur J Hum Genet. 2017;25:262–6.

21. Laquerriere A, Maluenda J, Camus A, Fontenas L, Dieterich K, Nolent F, et al. Mutations in CNTNAP1 and ADCY6 are responsible for severe arthrogryposis multiplex congenita with axoglial defects. Hum Mol Genet. 2014;23:2279–89.

22. Schuelke M, Oien NC, Oldfors A. Myopathology in the times of modern genetics. Neuropathol Appl Neurobiol. 2017;43:44–61.

23. Hedberg-Oldfors C, Lindgren U, Basu S, Visuttijai K, Lindberg C, Falkenberg M, et al. Mitochondrial DNA variants in inclusion body myositis characterized by deep sequencing. Brain Pathol. 2021;31:e12931.

24. Visuttijai K, Hedberg-Oldfors C, Lindgren U, Nordstrom S, Eliasdottir O, Lindberg C, et al. Progressive external ophthalmoplegia associated with novel MT-TN mutations. Acta Neurol Scand. 2021;143:103–8.

SUPPORTING INFORMATION

Additional supporting information may be found in the online version of the article at the publisher's website.
Supplementary Material
TABLE S1 Antibodies used in immunohistochemistry and western blot
FIGURE S1 Patient 1, quadriceps muscle at 4 months of age. There is increased variability of fibre size (A, H&E), multiple ragged red fibres and lipid vacuoles (B, Gomori trichrome) and profound COX deficiency (C, COX; D, COX-SDH) Bar = 50 μm
FIGURE S2 Patient 1, quadriceps muscle at 18 years of age. There is slight variability of fibre size (A, H&E), occasional ragged red fibres (B, Gomori trichrome) and numerous fibres with COX deficiency (C, COX; D, COX-SDH) Bar = 100 μm
FIGURE S3 Patient 2, quadriceps muscle at 2 months of age. There is increased variability of fibre size (A, H&E), multiple ragged red fibres and lipid vacuoles (B, Gomori trichrome) and profound COX deficiency (C, COX; D, COX-SDH) Bar = 50 μm
FIGURE S4 Patient 2, quadriceps muscle at 5 years of age. There is slight variability of fibre size and occasional central nuclei (A, H&E), no apparent ragged red fibres (B, Gomori trichrome) but occasional fibres with COX deficiency (C, COX) and occasional fibres with mitochondrial proliferation (D, SDH) Bar = 100 μm
FIGURE S5 Patient 2, quadriceps muscle at 14 years of age. There is marked variability of fibre size and numerous fibres with internal nuclei and a slight increase in connective tissue (A, H&E), no apparent ragged red fibres (B, Gomori trichrome) but numerous fibres with complete or partial COX deficiency (C, COX; D, COX-SDH) Bar = 100 μm
FIGURE S6 Patient 3, quadriceps muscle at 1 month of age. There is increased variability of fibre size (A, H&E), multiple ragged red fibres and lipid vacuoles (B, Gomori trichrome) and profound COX deficiency (C, COX; D, COX-SDH) Bar = 50 μm
FIGURE S7 Patient 4, quadriceps muscle at 4 months of age. There is increased variability of fibre size (A, H&E), multiple ragged red fibres and lipid vacuoles (B, Gomori trichrome) and profound COX deficiency (C, COX; D, COX-SDH) Bar = 50 μm
FIGURE S8 Patient 5, quadriceps muscle at 1 months of age. There is increased variability of fibre size (A, H&E), multiple ragged red fibres and lipid vacuoles (B, Gomori

trichrome) and profound COX deficiency (C, COX; D, COX-SDH) Bar = 50 μm

FIGURE S9 Patient 5, quadriceps muscle at 8 years of age. There is marked variability of fibre size, numerous necrotic and regenerating fibres and a slight increase in connective tisue (A and B, H&E), and numerous fibres with complete or partial COX deficiency (C, COX; D, COXSDH) Bar = 100 μm

FIGURE S10 Patient 6, quadriceps muscle at 9 years of age. There is slight variability of fibre size (A, H&E), and numerous fibres with mitochondrial proliferation and occasional ragged red fibres (B, Gomori trichrome). Occasional fibres with mitochondrial proliferation show partial COX deficiency (C, COX; D, COX-SDH) Bar = 100 μm

FIGURE S11 Patient 7, quadriceps muscle at 1 month of age. There is marked variability of fibre size (range: 5–40 μm) and marked increase in connective tissue (A, H&E; B, Gomori trichrome). Numerous fibres show partial or complete COX deficiency (C, COX; D, COXSDH) Bar = 50 μm

FIGURE S12 Repeated immunoblotting shows the same results with decreased levels of the complex I subunits NDUFB8 and NDUFS3 in P7. The decreased level of VDAC in P7 is also confirmed. Coomassie staining of the myosin heavy-chain band (MHc) serves as loading control. C, control, P, patient.

TABLE S2 Information about the 13 mtDNA encoded genes with the occurrence of the amino acid Glu